Unquenching effects on the coefficients of the Lüscher-Weisz action

Zh. Hao,[1] G. M. von Hippel,[2] R. R. Horgan,[3] Q. J. Mason,[3,4] and H. D. Trottier[1,5]

[1] *Department of Physics, Simon Fraser University, 8888 University Drive, Burnaby, British Columbia V5A 1S6, Canada*
[2] *Department of Physics, University of Regina, Regina, Saskatchewan S4S 0A2, Canada*
[3] *DAMTP, Centre for Mathematical Sciences, University of Cambridge, Cambridge CB3 0WA, United Kingdom*
[4] *Barclays Capital, 5 The North Colonnade, Canary Wharf, London E14 4BB, United Kingdom*
[5] *TRIUMF, 4004 Westbrook Mall, Vancouver, British Columbia V6T 2A2, Canada*

(Received 5 June 2007; published 30 August 2007)

The effects of unquenching on the perturbative improvement coefficients in the Symanzik action are computed within the framework of Lüscher-Weisz on-shell improvement. We find that the effects of quark loops are surprisingly large, and their omission may well explain the scaling violations observed in some unquenched studies.

DOI: 10.1103/PhysRevD.76.034507 PACS numbers: 12.38.Gc, 12.38.Bx

I. INTRODUCTION

The enormous advances in parallel computing made during the past few years, together with theoretical advances in the formulation of lattice gauge theories with fermions, have allowed lattice theorists to abandon the quenched approximation that dominated lattice QCD simulations for such a long time in favor of simulations using dynamical light quarks. This important step has allowed a significant reduction in systematic errors by removing the large and uncontrolled errors inherent in the quenched approximation.

The Fermilab Lattice, MILC and HPQCD collaborations have an ambitious program which to date has made several high-precision predictions from unquenched lattice QCD simulations [1,2], including accurate determinations of the strong coupling constant α_s [3], the light and strange quark masses [4], and the leptonic and semileptonic decays of the D meson [5]. To do this, we rely on the Symanzik-improved staggered-quark formalism [6], specifically the use of the asqtad [7] action. While this approach requires the use of the fourth root of the staggered-quark action determinant, all of the available evidence to date is consistent with the conclusion that the resulting theory is in the same universality class as continuum QCD, as long as the chiral limit is taken after the continuum limit [8].

Recent studies of the heavy-quark potential in full QCD [9] have shown an apparent increase in scaling violations compared to the quenched approximation, contrary to expectations. A possible reason for this would be that these scaling violations arise from the mismatch between the inclusion of sea quark effects in the simulation and the omission of sea quark effects in the improvement coefficients in the action, which would appear to spoil the $\mathcal{O}(a^2)$ improvement at the level of $\mathcal{O}(\alpha_s N_f a^2)$. A systematic study of $\mathcal{O}(\alpha_s a^2)$ effects is generally beyond the scope of the current perturbative improvement programme. Nevertheless, it is important to bring up-to-date the calculation by Lüscher and Weisz [10] and by Snippe [11] of the radiative correction to the $\mathcal{O}(a^2)$ tree-level Symanzik-improved gluon action to include the effects of dynamical quarks. This is important also because the Lüscher-Weisz improvement is currently included in many unquenched simulations [7]. Since the lattice spacing scale is set by measurement of the heavy-quark potential, there will be an induced $\mathcal{O}(\alpha_s N_f a^2)$ artifact by omitting the corrections due to unquenching. While such errors are generally smaller than other systematic errors in current state-of-the art studies, it is simple to remove them, using the result of the perturbative matching calculations done here, and this may prove advantageous in careful studies of different scale setting procedures.

In this paper, we present the determination of the lowest-order perturbative contributions from quark loops to the Symanzik improvement coefficients of the Lüscher-Weisz glue action. Including these contributions in future simulations, as well as accounting for their influence in the analysis of existing results, should help to eradicate the last remaining vestiges of the quenched approximation and any associated systematic errors from unquenched lattice results. Some of this work has been reported in preliminary form in [12].

II. CONCEPTS AND METHODS

First, let us briefly explain the ingredients of our calculation.

A. On-shell improvement

The original Symanzik improvement programme [13,14] aims to remove the discretization artifacts from the correlation functions of the lattice theory. For gauge theories, this has proven difficult to implement, since the correlation functions themselves are not gauge invariant. A way out of this difficulty is offered by the method of on-shell improvement introduced by Lüscher and Weisz [15,16] which aims to improve only gauge-invariant spectral quantities.

The Lüscher-Weisz action is given by [15,17]

$$S = \sum_x \Big\{ c_0 \sum_{\mu\neq\nu} \langle 1 - P_{\mu\nu}\rangle + 2c_1 \sum_{\mu\neq\nu} \langle 1 - R_{\mu\nu}\rangle + \tfrac{4}{3} c_2 \sum_{\mu\neq\nu\neq\rho} \langle 1 - T_{\mu\nu\rho}\rangle \Big\}, \quad (1)$$

where P, R and T are the plaquette, rectangle and "twisted" parallelogram loops, respectively.

The requirement of obtaining the Yang-Mills action in the continuum limit imposes the constraint

$$c_0 + 8c_1 + 8c_2 = 1, \quad (2)$$

which can be used to determine c_0 in terms of the other two coefficients. This leaves us with c_1 and c_2 as unknown coefficients which need to be determined in order to eliminate the $\mathcal{O}(a^2)$ lattice artifacts.

If we have two independent quantities Q_1 and Q_2 which can be expanded in powers of (μa), where μ is some energy scale, as

$$Q_i = \bar{Q}_i + w_i(\mu a)^2 + \mathcal{O}((\mu a)^4), \quad (3)$$

and which receive corrections

$$\Delta_{\text{imp}} Q_i = d_{ij} c_j (\mu a)^2 + \mathcal{O}((\mu a)^4) \quad (4)$$

from the improvement operators, then the $\mathcal{O}(a^2)$ matching condition reads

$$d_{ij} c_j = -w_i. \quad (5)$$

Since this equation is linear, we can decompose the w_i into a gluonic and a fermionic part as $w_i = w_i^{\text{glue}} + N_f w_i^{\text{quark}}$ and obtain the same decomposition for the c_i; thus, especially we do not need to repeat the quenched calculation [10,11] in order to obtain the $\mathcal{O}(N_f)$ contributions (however, doing so provides a useful check on the correctness of our methods, which we have performed successfully). At higher orders in perturbation theory, the d_{ij} and w_i will become functions of the c_i in lower orders.

At the tree-level, the fermions contribute nothing to gluonic observables, and hence the tree-level coefficients remain unchanged compared to the quenched case [10]:

$$c_1 = -\frac{1}{12}, \qquad c_2 = 0. \quad (6)$$

B. Lattice perturbation theory

Lattice field theory is usually employed as a nonperturbative regularisation; for the calculations we need to perform, however, we need a perturbative expansion of Lattice QCD.

In lattice perturbation theory, the link variables U_μ are expressed in terms of the gauge field A_μ as

$$U_\mu(x) = \exp(gaA_\mu(x + \tfrac{1}{2}\hat{\mu})), \quad (7)$$

which, when expanded in powers of g, leads to a perturbative expansion of the lattice action, from which the perturbative vertex functions can be derived.

The gauge field A_μ is Lie algebra-valued, and can be decomposed as

$$A_\mu(x) = \sum_a A_\mu^a(x) t^a, \quad (8)$$

with the t^a being anti-Hermitian generators of SU(N), where $N = 3$ in the case of QCD.

As in any perturbative formulation of a gauge theory, gauge fixing and ghost terms appear in the Fadeev-Popov Lagrangian; here we will not have to concern ourselves with these, since for the purpose of determining the unquenching effects at one loop we only need to consider quark loops. An additional term, which we also do not need to consider here, arises from the Haar measure on the gauge group.

The loop integrals of continuum perturbation theory are replaced by finite sums over the points of the reciprocal lattice in lattice perturbation theory, or integrals over the Brillouin zone where the lattice has infinite spatial extent.

To handle the complicated form of the vertices and propagators in lattice perturbation theory, we employ a number of automation methods [18–22] that are based on the seminal work of Lüscher and Weisz [10]. Three independent implementations by different authors have been used in this work to ensure against programming errors.

C. Twisted boundary conditions

We work on a four-dimensional Euclidean lattice of length La in the x and y directions and lengths $L_z a$, $L_t a$ in the z and t directions, respectively, where a is the lattice spacing and L, L_z, L_t are even integers. In the following, we will employ twisted boundary conditions [23] in much the same way as in [10,11]. The twisted boundary conditions we use for gluons and quarks are applied to the (x, y) directions and are given by $(\nu = x, y)$

$$U_\mu(x + L\hat{\nu}) = \Omega_\nu U_\mu(x) \Omega_\nu^{-1}, \quad (9)$$

$$\Psi(x + L\hat{\nu}) = \Omega_\nu \Psi(x) \Omega_\nu^{-1}, \quad (10)$$

where the quark field $\Psi_{sc}(x)$ becomes a matrix in smell-color space [24] by the introduction of a "smell" group SU(N_s) with $N_s = N$ in addition to the color group SU(N). We apply periodic boundary conditions in the (z, t) directions.

These boundary conditions lead to a change in the Fourier expansion of the fields which now reads

$$A_\mu(x) = \frac{1}{NL^2 L_z L_t} {\sum_p}' \Gamma_p e^{ipx} \tilde{A}_\mu(p), \quad (11)$$

$$\Psi_\alpha(x) = \frac{1}{NL^2L_zL_t}\sum_p \Gamma_p e^{ipx}\tilde{\Psi}_\alpha(x). \tag{12}$$

In the twisted (x, y) directions the sums are over

$$p_\nu = mn_\nu, \qquad -\frac{NL}{2} < n_\nu \leq \frac{NL}{2}, \qquad \nu = (x, y), \tag{13}$$

where $m = \frac{2\pi}{NL}$, and in the untwisted (z, t) directions the sums are over

$$p_\nu = \frac{2\pi}{L_\nu}n_\nu, \qquad -\frac{L_\nu}{2} < n_\nu \leq \frac{L_\nu}{2}, \qquad \nu = (z, t). \tag{14}$$

The modes with $(n_x = n_y = 0 \bmod N)$ are omitted from the sum in the case of the gluons since the gauge group is non-Abelian, and this is signified by the prime on the summation symbol in Eq. (11). In particular, this removes the zero mode from the gluon spectrum and so the mass-scale m defined above acts as a gauge-invariant infrared regulator. The matrices Γ_p are given by (up to an arbitrary phase, which may be chosen for convenience)

$$\Gamma_p = \Omega_x^{-n_y}\Omega_y^{n_x}. \tag{15}$$

The momentum sums for quark loops need to be divided by N to remove the redundant smell factor.

The twisted theory can be viewed as a two-dimensional field theory in the infinite (z, t) plane with the modes in the twisted directions being considered in the spirit of Kaluza-Klein modes. Denoting $\mathbf{n} = (n_x, n_y)$, the stable particles in the (z, t) continuum limit of this effective theory are called the A mesons ($\mathbf{n} = (1, 0)$ or $\mathbf{n} = (0, 1)$) with mass m and the B mesons ($\mathbf{n} = (1, 1)$) with mass $\sqrt{2}m$ [11].

D. Small-mass expansion

To extract the $\mathcal{O}(a^2)$ lattice artifacts, we first expand some observable quantity Q in powers of ma at fixed $m_q a$:

$$Q(ma, m_q a) = a_0^{(Q)}(m_q a) + a_2^{(Q)}(m_q a)(ma)^2 + \mathcal{O}((ma)^4, (ma)^4\log(ma)), \tag{16}$$

where the coefficients in the expansion are all functions of $m_q a$. There is no term at $\mathcal{O}((ma)^2\log(ma))$ since the gluon action is improved at tree-level to $O(a^2)$ [11]. Since we wish to extrapolate to the chiral limit it might be thought that we can set $m_q a = 0$ straight away to achieve this end. However, the correct chiral limit is $m_q a \to 0$, $ma \to 0$, $m_q/m > C$, where $m = \frac{2\pi}{NL}$ as before and C is a constant determined by the requirement that the appropriate Wick rotation can be performed in order to evaluate the Feynman integrals. If the inequality is violated this results in a pinch singularity. It is physically sensible that the correct limit is $L \to \infty$ before $m_q \to 0$ since this divorces the two infrared scales and avoids complication. This does, however, require us to consider the double expansion in $m_q a$, ma and carry out the extrapolation to $m_q a = 0$ for the coefficients in Eq. (16). We return to this issue in the next section when we discuss choice of integration contours.

To extrapolate to the chiral limit, $m_q a \to 0$, we will fit the coefficients in the expansion for Q in ma to their most general expansion in $m_q a$ for small $m_q a$.

For $a_0^{(Q)}(m_q a)$ we have

$$a_0^{(Q)}(m_q a) = b_{0,0}^{(Q)}\log(m_q a) + a_{0,0}^{(Q)}. \tag{17}$$

Since we expect a well-defined continuum limit, $a_0^{(Q)}(m_q a)$ cannot contain any negative powers of $m_q a$ but, depending on the quantity Q, it may contain logarithms; $b_{0,0}^{(Q)}$ is the continuum anomalous dimension associated with Q which is determined by a continuum calculation.

There can be no terms in $(m_q a)^{2n}$, $n > 0$ since these are obviously nonzero in the limit $ma \to 0$, and there is no counterterm in the gluon action that can compensate for a scaling violation of this kind.

For $a_2^{(Q)}(m_q a)$ we find

$$a_2^{(Q)}(m_q a) = \frac{a_{2,-2}^{(Q)}}{(m_q a)^2} + a_{2,0}^{(Q)} + (a_{2,2}^{(Q)} + b_{2,2}^{(Q)}\log(m_q a)) \times (m_q a)^2 + \mathcal{O}((m_q a)^4). \tag{18}$$

After multiplication by $(ma)^2$ the $(m_q a)^{-2}$ contribution gives rise to a continuum contribution to Q, and $a_{2,-2}^{(Q)}$ is calculable in continuum perturbation theory. There can be no term in $(m_q a)^{-2}\log(m_q a)$ since this would be a volume-dependent further contribution to the anomalous dimension of Q, and there can be no term in $\log(m_q a)$ since the action is tree-level $O(a^2)$ improved [13].

Depending on the choice of observable Q there may be additional constraints on the coefficients which appear in the expansions. We discuss these in the next section in the context of the particular observables with which we concern ourselves.

III. CALCULATIONS AND RESULTS

In this section we lay out the calculation of the unquenching effects to order $\mathcal{O}(\alpha_s N_f a^2)$. The numbers and quantities given in the following are per quark flavor, and hence need to be multiplied by N_f throughout.

A. The A meson mass

The simplest spectral quantity that can be chosen within the framework of the twisted boundary conditions outlined above is the (renormalized) mass of the A meson. In agreement with Eq. (109) of [11] the one-loop correction to the A meson mass (for A mesons with positive spin) is given by

$$m_A^{(1)} = -Z_0(\mathbf{k})\frac{\pi_{11}^{(1)}(k)}{2m_A^{(0)}}\Bigg|_{k=(im_A^{(0)},0,m,0)} \tag{19}$$

where $Z_0(\mathbf{k}) = 1 + \mathcal{O}((ma)^4)$ is the residue of the pole of the tree-level gluon propagator at spatial momentum $\mathbf{k}$, and $m_A^{(0)}$ is defined so that the momentum k is on-shell. We consider the dimensionless quantity $m_A^{(1)}/m$. The fermionic diagrams that contribute to this quantity are shown in Fig. 1.

The anomalous dimension of m_A is zero and so using Eq. (17) we have

$$b_{0,0}^{(m_A,1)} = 0. \tag{20}$$

Using physical arguments we can determine the behavior of other coefficients. From continuum calculations we find

$$a_{2,-2}^{(m_A,1)} = 0. \tag{21}$$

This result follows from the fact that the fermion contribution at one-loop order to m_A is IR finite since the fermion has a nonzero mass and is 4D Lorentz invariant. Thus, $a_{2,-2}^{(m_A)}$ can be constructed only from 4D Lorentz invariants of which we have only $\boldsymbol{\epsilon}_A \cdot \mathbf{k}_A$ and $\mathbf{k}_A^2$, where $\boldsymbol{\epsilon}_A$ is the A-meson polarization vector. However, gauge invariance implies $\boldsymbol{\epsilon}_A \cdot \mathbf{k}_A = 0$ and the on-shell condition gives $\mathbf{k}_A^2 = 0$ and so, there being no nonzero Lorentz invariant, we deduce the result.

A much less obvious deduction is that $a_0^{(m_A,1)}(m_q a) = 0$, which together with Eqs. (17) and (20) implies that $a_{0,0}^{(m_A,1)} = 0$. A necessary ingredient to derive this result is the fact that the one-loop fermion contribution to m_A is IR finite in the limit $m \to 0$ ($L \to \infty$) since the fermion mass, m_q, is nonzero. We thus expect that in this limit Lorentz invariance will be restored, although for L finite this will not be the case. Gauge invariance and the Ward Identity then ensure that, in this limit, Lorentz invariance implies that the gluon self-energy function $\pi_{\mu\nu}(\mathbf{k})$ satisfies

$$\pi_{\mu\nu}(\mathbf{k}) = (k^2 g_{\mu\nu} - k_\mu k_\nu)\pi(k^2). \tag{22}$$

From [10,11] the one-loop contribution to m_A is proportional to $\boldsymbol{\epsilon}^\mu \boldsymbol{\epsilon}^\nu \pi_{\mu\nu}(\mathbf{k})$. In the limit $L \to \infty$ we are able to use Eq. (22) and we find that this contribution is zero by gauge invariance and the on-shell condition $k^2 = 0$. In contrast, the contribution to $a_0^{(m_A)}$ from internal gluon loops is not zero by this argument; it is indeed calculated in [10,11]. The reason is that the one-loop gluon contribution is not IR finite in the $m \to 0$, $L \to \infty$ limit since the IR-regulating mass is m; the internal gluon "feels" the finite boundary of the lattice in the x, y direction no matter how large L is. Consequently, we cannot expect to use restoration of Lorentz invariance to limit the form that the purely gluonic $\pi_{\mu\nu}(\mathbf{k})$ takes, and so no deduction concerning this coefficient can be made.

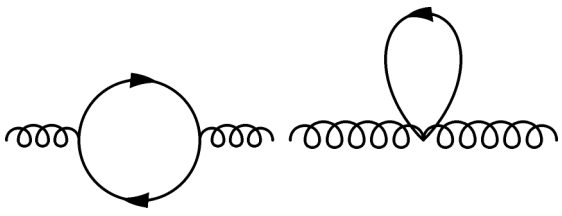

FIG. 1. The fermionic one-loop diagrams contributing to the A meson mass renormalization as well as to the wave-function renormalization for A and B mesons.

An alternative explanation for why $a_0^{(m_A,1)} = 0$ also relies on the restoration of Lorentz invariance in the $m \to 0$ limit. In this limit, the action is isotropic with metric tensor $g_{\mu\nu} = \mathrm{diag}(1, 1, 1, 1)$. However, the twisted boundary conditions break Lorentz invariance and single out the twisted x, y directions, and so we must expect that radiative corrections will renormalize $g_{\mu\nu}$ in a way that can break Lorentz symmetry. The mass shell condition for the A-meson is then

$$g_{\mu\nu}^R k^\mu k^\nu = 0, \qquad k_\mu = (ip_0, 0, m, k_3), \tag{23}$$

where g^R is the renormalized metric tensor. This is reinterpreted as a renormalization of the A-meson mass m with

$$m_A^R = \frac{g_{11}^R(m)}{g_{11}} m. \tag{24}$$

This can also be interpreted as an anisotropy renormalization. Since the one-loop fermion contribution is IR finite and Lorentz symmetry is restored in the limit $m \to 0$ we then have that $g_{11}^R(m = 0) = g_{11} = 1$ and m_A is not renormalized. This is not the case for the one-loop gluon contribution, which is not IR finite, and so the assumption that Lorentz symmetry is restored as $m \to 0$ is incorrect.

For the kinematics used here this means that in the limit $m \to 0$, $L \to \infty$ then π_{11} vanishes and hence from Eq. (19) so does $m_A^{(1)}/m$. This expectation is accurately verified by our calculation: the extrapolation of $m_A^{(1)}/m$ to $m = 0$ indeed gives zero (cf. Fig. 2).

In the chiral limit $m_q \to 0$, the term w_i that appears on the right-hand side of Eq. (5) is $a_{2,0}^{(Q)}$, and it is this limit and this coefficient that we will concern ourselves with hereafter.

The $\mathcal{O}(\alpha_s(ma)^2)$ contribution from improvement of the action is given by [11]

$$\Delta_{\mathrm{imp}} \frac{m_A^{(1)}}{m} = -(c_1^{(1)} - c_2^{(1)})(ma)^2 + \mathcal{O}((ma)^4) \tag{25}$$

leading to the improvement condition

$$c_1^{(1)} - c_2^{(1)} = a_{2,0}^{(m_A,1)}. \tag{26}$$

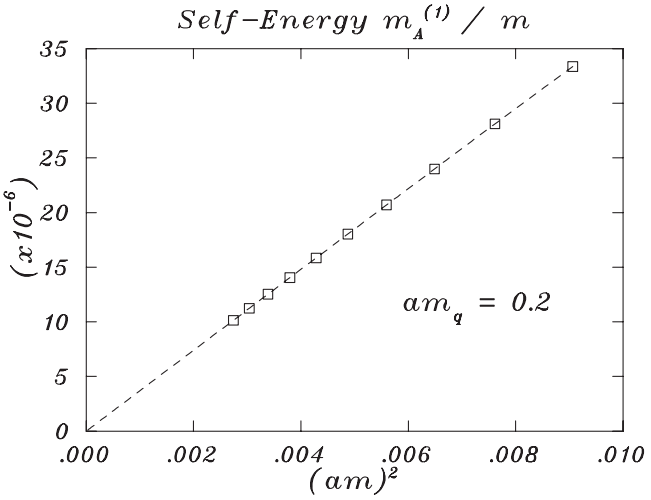

FIG. 2. A plot of the fermionic contributions to the one-loop A meson self-energy $m_A^{(1)}/m$ against $(ma)^2$. The vanishing of $m_A^{(1)}/m$ in the infinite-volume limit can be seen clearly.

B. The three-point coupling

An effective coupling constant λ for an AAB meson vertex is defined as

$$\lambda = g_0\sqrt{Z(\mathbf{k})Z(\mathbf{p})Z(\mathbf{q})}e_j\Gamma^{1,2,j}(k, p, q), \tag{27}$$

where we have factored out a twist factor of $\frac{i}{N}\,\mathrm{Tr}([\Gamma_k, \Gamma_p]\Gamma_q)$ from both sides, and the momenta and polarizations of the incoming particles are

$$\begin{aligned} k &= (iE(\mathbf{k}), \mathbf{k}); \qquad \mathbf{k} = (0, m, ir) \\ p &= (-iE(\mathbf{p}), \mathbf{p}); \qquad \mathbf{p} = (m, 0, ir) \\ q &= (0, \mathbf{q}); \qquad \mathbf{q} = (-m, -m, -2ir) \\ e &= (0, 1, -1, 0). \end{aligned} \tag{28}$$

Here $r > 0$ is defined such that $E(\mathbf{q}) = 0$. This coupling is a spectral quantity since it can be related to the scattering amplitude of A mesons [16]. We expand Eq. (27) perturbatively to one-loop order and find in agreement with Eq. (137) of [11]:

$$\begin{aligned} \frac{\lambda^{(1)}}{m} = (1 - \tfrac{1}{24}m^2)\frac{\Gamma^{(1)}}{m} - \frac{4}{k_0}\frac{d}{dk_0}\pi_{11}^{(1)}(k)\Big|_{k_0=iE(\mathbf{k})} \\ - (1 - \tfrac{1}{12}m^2)\frac{d^2}{dq_0^2}(e^i e^j \pi_{ij}^{(1)}(q))\Big|_{q_0=0} + \mathcal{O}(m^4). \end{aligned} \tag{29}$$

The fermionic diagrams contributing to the irreducible three-point function $\Gamma^{(1)}$ are shown in Fig. 3. Using Eq. (17) and the known anomalous dimension of the coupling constant we have

$$b_{0,0}^{(\lambda,1)} = -\frac{N_f}{3\pi^2}g^2. \tag{30}$$

Unlike the argument for $a_{2,-2}^{(m_A,1)} = 0$ above, a continuum calculation gives

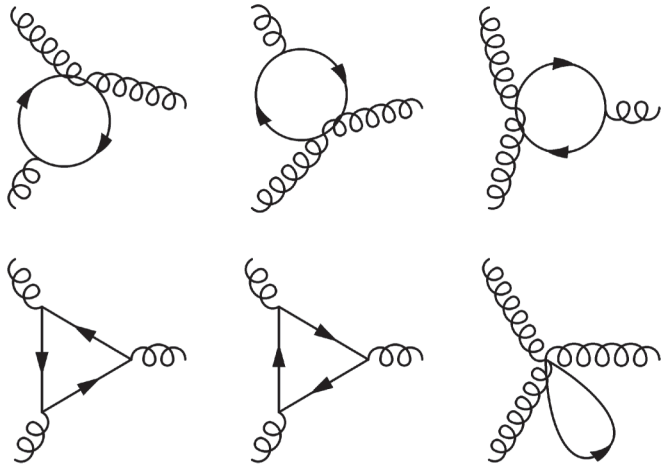

FIG. 3. The fermionic one-loop diagrams contributing to the three-point function.

$$a_{2,-2}^{(\lambda,1)} = -\frac{N_f}{120\pi^2}g^2. \tag{31}$$

In this case there are nonzero Lorentz invariants for the three-point function such as $\boldsymbol{\epsilon}_A \cdot \mathbf{k}_B$ etc. and so we expect this coefficient to be nonzero.

The improvement contribution to λ is [11]

$$\Delta_{\mathrm{imp}}\frac{\lambda^1}{m} = 4(9c_1^{(1)} - 7c_2^{(1)})(ma)^2 + \mathcal{O}((ma)^4) \tag{32}$$

leading to the improvement condition

$$4(9c_1^{(1)} - 7c_2^{(1)}) = -a_{2,0}^{(\lambda,1)}. \tag{33}$$

Tests of our calculation are that the fit for $a_{0,0}^{(\lambda,1)}$ must give the correct anomalous dimension stated in Eq. (30), and that our fits reproduce the continuum result $a_{2,-2}^{(\lambda,1)} = -g^2/120\pi$. Both are accurately verified (cf. Figs. 4 and 5).

C. Choice of integration contours

The external lines of the diagrams are on their respective mass shells but with complex three-momentum $\mathbf{k}$ in which the third component, k_3, has been continued to an imaginary value parametrized by the variable r as shown in Eq. (28); in the Euclidean formulation k_0 is also imaginary. In evaluating the loop integrals that are not pure tadpoles, care must be taken to ensure that the amplitudes calculated are the correct analytic continuations in r from the Minkowski space on-shell amplitudes defined with real three-momenta to the ones in Eq. (28).

The situation is complicated by the presence of two mass scales m, m_q. The integrals are evaluated after performing a Wick rotation in k_0, taking care to avoid contour crossing of any poles that move as r is continued from $r = 0$ to $r = m/\sqrt{2}$. We find that m_q/m must be chosen larger than a

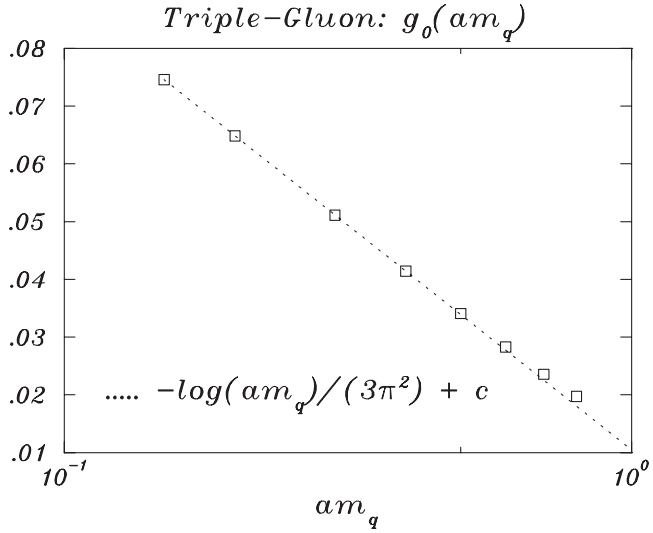

FIG. 4. A plot of $a_0^{(\lambda,1)}$ against $m_q a$ which shows the agreement between the numerical lattice results and the known anomalous dimension.

minimum value, dependent on the graph being considered, to avoid any contour being pinched. The outcome is that after the Wick rotation in k_0, the (Euclidean) integration contour for either k_0 or, in one case, k_3 must be shifted by an imaginary constant.

We find it sufficient that for the calculation of $m_A^{(1)}$ and $Z_A(k)$ we impose $m_q > m/2$ and for $\Gamma^{(1)}$ and $Z_B(q)$ that $m_q > m/\sqrt{2}$.

D. Extracting the coefficients

To extract the improvement coefficients from our diagrammatic calculations, we compute the diagrams for a number of different values of both L and m_q with $N_f = 1$,

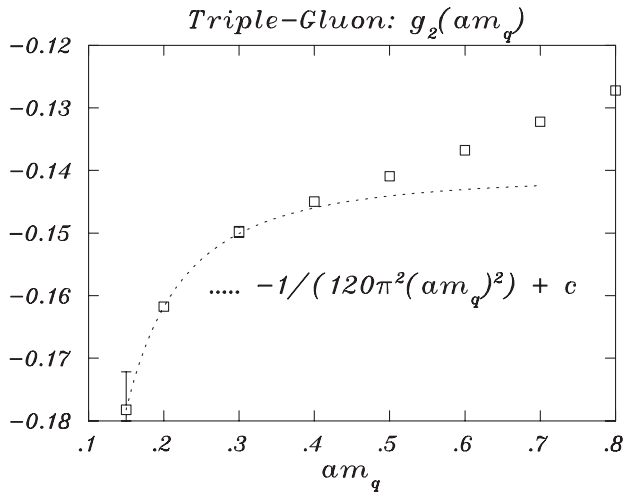

FIG. 5. A plot of $a_2^{(\lambda,1)}$ against $m_q a$ with the analytical continuum result for the infrared divergence shown for comparison.

TABLE I. The coefficients from the fits of $m_A^{(1)}$ and $\lambda^{(1)}/m$ against ma.

$m_q a$	$a_2^{(m_A,1)}$	$a_0^{(\lambda,1)}$	$a_2^{(\lambda,1)}$
0.15	0.003 675 2(7)	0.074 56(1)	−0.178(6)
0.2	0.003 701(1)	0.064 816 1(5)	−0.1617(4)
0.3	0.003 730 711(1)	0.051 090(2)	−0.1498(9)
0.4	0.003 729 96(4)	0.041 433 2(1)	−0.144 98(6)
0.5	0.003 696 507(2)	0.034 085 72(2)	−0.140 933(7)
0.6	0.003 632 867 1(4)	0.028 272 563(9)	−0.136 776(2)
0.7	0.003 543 542 9(3)	0.023 575 013(4)	−0.132 222(1)
0.8	0.003 433 769 0(4)	0.019 733 513(1)	−0.127 22(3)
0.9	0.003 308 797 1(2)	—	—
1.0	0.003 173 470 0(3)	—	—
1.2	0.002 888 2(3)	0.009 976(2)	−0.1044(1)

$N = 3$. At each value of m_q, we then perform a fit in ma of the form given in Eq. (16) to extract the coefficients $a_n^{(Q,1)}(m_q a)$, $n = 0, 2$. The results of these fits are given in Table I.

To facilitate our fits, we make use of the prior physical knowledge we have: In the case of $m_A^{(1)}$, we have $a_0^{(m_A,1)} = 0$ because of gauge invariance.

Performing a fit of the form (17) and (18), respectively, on these coefficients, we get the required coefficients of the $\mathcal{O}(a^2)$ lattice artifacts in the chiral limit to be

$$a_{2,0}^{(m_A,1)} = 0.003\,61(1) \tag{34}$$

$$a_{2,0}^{(\lambda,1)} = -0.140(1) \tag{35}$$

These coefficients are to be identified with the w_i of Eq. (5).

Here, again, we have facilitated our fits by making use of our prior knowledge: For $m_A^{(1)}$, $a_{2,-2}^{(m_A,1)}$ vanishes, and for $\lambda^{(1)}$, we have two known continuum contributions: $b_{0,0}^{(\lambda,1)} = -1/3\pi^2$ is the one-loop coefficient of the β-function and $a_{2,-2}^{(\lambda,1)} = -1/120\pi^2$ is the continuum coefficient of the infrared divergence m^2/m_q^2.

Solving Eqs. (26) and (33) for $c_i^{(1)}$, our results can be summarized as

$$c_1^{(1)} = -0.025\,218(4) + 0.004\,86(13)N_f, \tag{36}$$

$$c_2^{(1)} = -0.004\,418(4) + 0.001\,26(13)N_f, \tag{37}$$

where the quenched ($N_f = 0$) results are taken from [11].

IV. CONCLUSIONS

Repeating the analysis of [17] and using their notation we express the radiatively corrected action of Eq. (1) as [15,17]

$$S[U] = \sum_{i=0}^{2} \beta_i S_i[U]. \tag{38}$$

Then

$$\beta_1 = -\frac{\beta_0}{20u_0^2}\left[1 - \left(\frac{12\pi}{5}c_0^{(1)} + 48\pi c_1^{(1)} + 2u_0^{(1)}\right)\alpha_s\right],$$
$$\beta_2 = \frac{12\pi\beta_0}{5u_0^2}c_2^{(1)}\alpha_s. \tag{39}$$

The quenched radiative contributions have been analyzed in [17] and so we may write

$$\beta_1 = -\frac{\beta_0}{20u_0^2}\left[1 + 0.4805\alpha_s - \left(\frac{12\pi}{5}c_{0,f}^{(1)} + 48\pi c_{1,f}^{(1)}\right)\alpha_s\right],$$
$$\beta_2 = -\frac{\beta_0}{u_0^2}\left(0.033\alpha_s - \frac{12\pi}{5}c_{2,f}^{(1)}\alpha_s\right), \tag{40}$$

where now all the one-loop coefficients $c_{i,f}^{(1)}$ contain only quark loop contributions.

Plugging in the numbers obtained in this work we find

$$\beta_1 = -\frac{\beta_0}{20u_0^2}[1 + 0.4805\alpha_s - 0.3637(14)N_f\alpha_s],$$
$$\beta_2 = -\frac{\beta_0}{u_0^2}(0.033\alpha_s - 0.009(1)N_f\alpha_s). \tag{41}$$

With $N_f = 3$ the shift from the quenched values is surprisingly large, and may have a significant impact; especially, it may explain the increased scaling violations seen in some unquenched simulations.

ACKNOWLEDGMENTS

The authors thank Fermilab for the use of computing resources. This work was supported in part by the Canadian Natural Sciences and Engineering Research Council (NSERC), the government of Saskatchewan, and the U.K. Particle Physics and Astronomy Research Council (PPARC).

[1] C. T. H. Davies *et al.*, Phys. Rev. Lett. **92**, 022001 (2004).
[2] C. Aubin *et al.*, Phys. Rev. D **70**, 114501 (2004).
[3] Q. Mason *et al.*, Phys. Rev. Lett. **95**, 052002 (2005).
[4] Q. Mason, H. D. Trottier, R. Horgan, C. T. H. Davies, and G. P. Lepage, Phys. Rev. D **73**, 114501 (2006).
[5] A. S. Kronfeld *et al.*, Proc. Sci., LAT2005 (2006) 206 [arXiv:hep-lat/0509169].
[6] G. P. Lepage, Phys. Rev. D **59**, 074502 (1999).
[7] K. Orginos, D. Toussaint, and R. L. Sugar, Phys. Rev. D **60**, 054503 (1999).
[8] S. R. Sharpe, Proc. Sci., LAT2006 (2006) 022 [arXiv:hep-lat/0610094].
[9] C. T. H. Davies (private communication).
[10] M. Lüscher and P. Weisz, Nucl. Phys. **B266**, 309 (1986).
[11] J. Snippe, Nucl. Phys. **B498**, 347 (1997).
[12] Zh. Hao, MS thesis, Simon Fraser University, 2006.
[13] K. Symanzik, Nucl. Phys. **B226**, 187 (1983).
[14] K. Symanzik, Nucl. Phys. **B226**, 205 (1983).
[15] M. Lüscher and P. Weisz, Commun. Math. Phys. **97**, 59 (1985).
[16] M. Lüscher and P. Weisz, Phys. Lett. **158B**, 250 (1985).
[17] M. G. Alford, W. Dimm, G. P. Lepage, G. Hockney, and P. B. Mackenzie, Phys. Lett. B **361**, 87 (1995).
[18] I. T. Drummond, A. Hart, R. R. Horgan, and L. C. Storoni, Nucl. Phys. B, Proc. Suppl. **119**, 470 (2003).
[19] A. Hart, G. M. von Hippel, R. R. Horgan, and L. C. Storoni, J. Comput. Phys. **209**, 340 (2005).
[20] M. A. Nobes, H. D. Trottier, G. P. Lepage, and Q. Mason, Nucl. Phys. B, Proc. Suppl. **106**, 838 (2002).
[21] M. A. Nobes and H. D. Trottier, Nucl. Phys. B, Proc. Suppl. **129**, 355 (2004).
[22] H. D. Trottier, Nucl. Phys. B, Proc. Suppl. **129**, 142 (2004).
[23] G. 't Hooft, Nucl. Phys. **B153**, 141 (1979).
[24] G. Parisi, Summer Inst. Progress in Gauge Field Theory, Cargese, France, 1983.